Characterisation of antagonistically actuated, stiffness-controllable joint-link units for cobots

Wenlong Gaozhang[1], Jialei Shi[1], Yue Li[2], Agostino Stilli[3], Helge Wurdemann[1]

***Abstract*— Soft robotic structures may play a major role in the 4th industrial revolution. Researchers have successfully demonstrated some of the advantages of soft robotics over traditional robots made of rigid links and joints in several application areas. In some applications, robots will need to work closely together with humans in a safe manner. However, soft robots have limited ability to exert larger forces when it comes to interaction with the environment, hence, changing their stiffness on-demand over a wide range. Variable stiffness links (VSL) and joints (VSJ) have been investigated to achieve on-demand forces and, at the same time, be inherently safe in interactions with humans.**

This paper investigates the influence of antagonistically actuated, stiffness-controllable joint-link units (JLUs) on the performance of collaborative robots (i.e. stiffness, load capacity, repetitive accuracy) and characterizes the difference compared with rigid units. A JLU is made of a combination of a VSL, a (VSJ) and their rigid counterparts. Experimental results show that the VSL has minor differences in terms of stiffness ($0.62 \sim 0.95$), output force ($0.93 \sim 0.94$) and repetitive accuracy compared with the rigid link. For the VSJ, our results show a significant gap compared with the servo motor with regards to maximum stiffness ($0.14 \sim 0.21$) and repetitive position accuracy ($0.07 \sim 0.25$). However, similar performance on repetitive force accuracy and better performance on the maximum output force ($1.54 \sim 1.55$ times) are demonstrated.

I. Introduction

Notable advances in soft material robotics have successfully demonstrated their advantages over traditional rigid-linked robots [1]. However, challenges on how to exert on-demand forces onto objects or the environment remain [2]. In recent years, one method of achieving on-demand forces includes the integration of soft, variable stiffness components [3]. For collaborative robots (cobots), these types of components allow the exertion of increasing forces and, at the same time, realize inherently safe human-robot interaction [4]. Researchers have investigated many soft components for allowing stiffness-controllability in links and joints/actuators [5]–[10]. For instance, a stiffness-controllable link [11], [12] was proposed to replace the rigid link in currently available collaborative robots. The link is effectively a cylindrical sleeve made of a composite of

*This work is supported by the Engineering and Physical Sciences Research Council (grant numbers: EP/R037795/1, EP/S014039/1 and EP/V01062X/1) and by UCL Mechanical Engineering.

[1]W. Gaozhang, J. Shi and H.A. Wurdemann are with the Department of Mechanical Engineering, University College London, UK. h.wurdemann@ucl.ac.uk

[2]Y. Li is with the School of Biomedical Engineering & Imaging Sciences (BMEIS), King's College London, UK. yue.3.li@kcl.ac.uk

[3]A. Stilli is with the Department of Medical Physics and Biomedical Engineering, University College London, UK. a.stilli@ucl.ac.uk

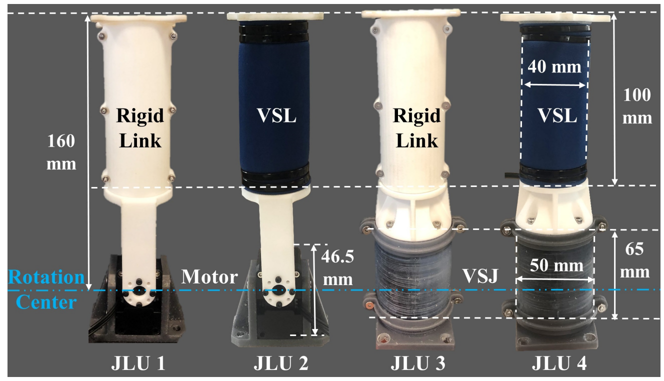

Fig. 1. A set of four joint-link units (JLUs) have been designed, manufactured and compared: a Dynamixel XM430 servo motor (CA, USA) and a rigid link manufactured by SLS 3D printing process with the material of Nylon PA2200 (JLU 1), a motor and a variable stiffness link (VSL) (JLU 2), a variable stiffness joint (VSJ) and rigid link (JLU 3), a VSJ and a VSL (JLU 4). All of these four JLUs have the same rotation centre. The distance between between the rotational centres to the tip of the JLUs is 160 mm, while the length of the VSL and the rigid link is 100 mm.

fabric and silicone material. By air pressurization, omnidirectional stiffness variation can be achieved. On the other hand, modeling approaches have been proposed to control the compliance of this kind of links [13], [14]. Besides, variable stiffness joints driven by soft actuators have been increasingly explored [15]–[17]. Output torque variation of these joints can be achieved through the design of rotational structures which position and stiffness are proportionally changing depending on the inner fluidic pressure [18]–[20]. These cobots equipped with variable stiffness joints driven by soft actuators can exert on-demand stiffness/force and, at the same time, guarantee inherently safe human-robot interaction.

However, it has not yet been understood how different soft, variable stiffness components affect the performance (i.e. stiffness, load capacity, and motion accuracy) of collaborative robots compared with rigid components. In particular, a comparison and evaluation of different components such as a link versus joint/actuator or a combination of both have not yet been investigated.

This paper investigates the influence of antagonistically actuated, stiffness-controllable joint-link units (JLUs) on the performance of collaborative robots (i.e. stiffness, load capacity, accuracy), and characterizes the difference compared with rigid units. A JLU is made of a combination of a variable stiffness link (VSL, building on our previous work [11], [12]), a rotational variable stiffness joint (VSJ)

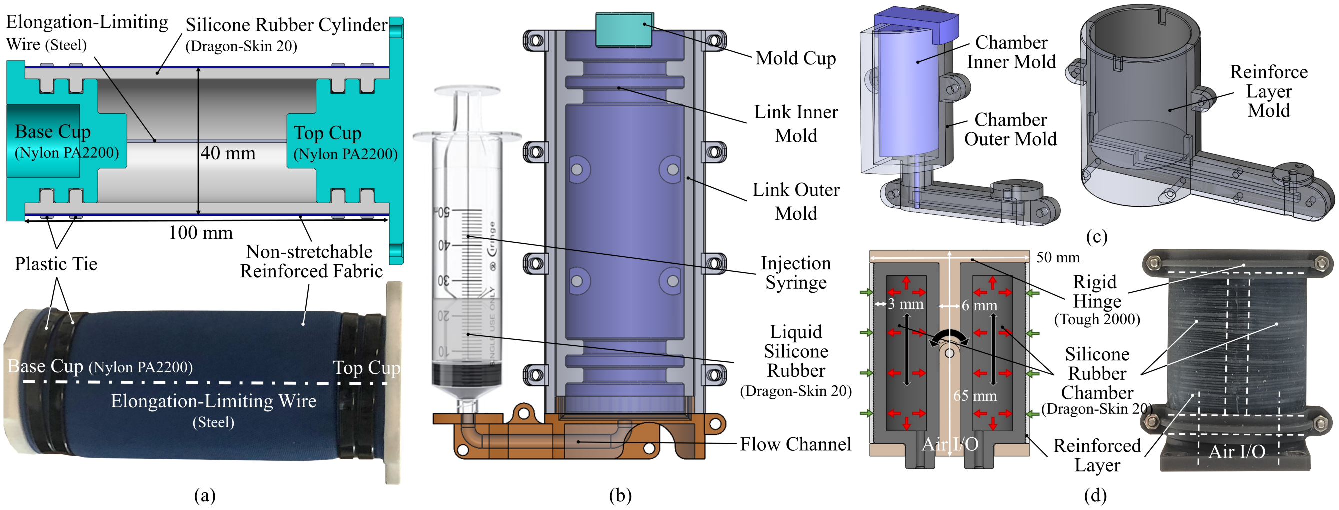

Fig. 2. (a) Sectional CAD drawing (top) and physical prototype (bottom) of the variable stiffness link (VSL). A silicone-based cylinder, which is reinforced by fabric material, is sealed by two caps. Pressurized air can inflate or deflate in the VSL, leading to omnidirectional stiffness variation. The non-stretchable reinforced fabric surrounding the cylinder wall tightly is used to prevent any radial extension, while the elongation-limiting wire between the top and base cap maintains the length of the link during pressurization. A VSL has a 40 mm diameter with a 100 mm length. (b) Injection molds used to manufacture the silicone shell of the VSL. (c) Injection molds used to manufacture the silicone chambers for the variable stiffness joint (VSJ). (d) Sectional CAD drawing (left) and physical prototype (right) of the VSJ. Two silicone chambers are located on both sides of a rigid central hinge. A layer of reinforced fabric thread is wrapped around the circumference of the VSJ preventing any radial expansion. A VSJ has a 50 mm diameter with a 65 mm length.

and their rigid counterparts. As shown in 1, we set a unit composed of a Dynamixel XM430 servo motor and a rigid link manufactured by the SLS 3D printing process with the material of Nylon PA2200 (JLU 1) representing the traditional rigid JLU of collaborative robots. The other three units are composed of at least one soft, stiffness-controllable components: a motor joint and a VSL (JLU 2), a VSJ and a rigid link (JLU 3) as well as a VSJ and VSL (JLU 4), respectively. We carried out a set of characterization experiments evaluating the stiffness, load capacity, and repetitive accuracy of these four JLUs. The results of the experiments highlight the difference between rigid components and soft, variable stiffness components, demonstrating the feasibility of building JLUs made of one or two soft, variable stiffness components for constructing collaborative robots as well as providing valuable guidance for the design and modification of soft, variable stiffness components.

II. Design and Integration of Joint-Link Units (JLUs)

A. The omnidirectional variable stiffness link (VSL)

Based on our previous work [11], [12], [21], a new version of the omnidirectional variable stiffness link (VSL) has been fabricated for this work allowing modularity when building sets of stiffness-controllable joint-link units (JLUs). The VSL consists of a cylindrical shell made of a silicone/fabric composite and a 1 mm diameter elongation-limiting steel wire between the top and base cap as shown in Fig. 2 (a). The silicone layer is made of the Dragon-Skin 20 (Smooth-On, Easton, PA, USA) with an elongation rate of 620% and tensile strength of 550 psi. The fabric is made of canvas fabric with a 1 mm thickness and sewed using cotton thread into a cylindrical shape. The cylindrical shell is tightened to the caps by plastic ties. Input of pressurized air will lead to an increase in stiffness as the volume of the VSL is constrained by the fabric material. The non-stretchable reinforced fabric tightly surrounding the cylinder wall is used to prevent any radial extension, while the elongation-limiting wire in the centre maintains the length of the link. In order to allow modularity of different JLU components (a Dynamixel XM430 servo motor, a rigid link and the variable stiffness joint (VSJ)), the VSL has a 40 mm diameter with a 100 mm length. The VSL has been manufactured utilizing injection molding. The molds are shown in Fig. 2 (b). The injection molding process minimizes any air bubbles remaining in the silicone during molding procedure.

B. The rotational variable stiffness joint (VSJ)

To achieve variable stiffness capability of our soft robotic joint VSJ, we designed and manufactured two silicone-based chambers and a rigid central hinge as shown in Fig. 2 (d). The silicone-based chambers are located on each side of the hinge, opposing each other. These chambers can be pressurized by compressed air, so that they will elongate pushing the tip of the hinge and resulting in a rotation motion. Stiffness can then be achieved by pressurisation of both chambers simultaneously in an antagonistic way. The thickness of the hinge is 6 mm. The walls of the actuation chambers are 3 mm thick. For the fabrication of the silicone-based actuation chamber, the injection molding process was utilized using Dragon-Skin 20 silicone rubber material (Smooth-On, Easton, PA, USA). Dragon-Skin 20 has an elongation rate of 620% and tensile strength of 550 psi. The molds are shown in Fig. 2 (c). The central hinge is made by a 3D printing process (SLA, Formlabs, Berlin, Germany) using Tough2000 material. The two chambers and central hinge are then assembled, while non-extensible cotton fabric thread is twined around the entire circumference to create a reinforced layer. The outside wall mold is then used to create a silicone wall for the joint, fixing the position of and gaps between the reinforcement layer. The overall dimension of the VSJ is shown in Fig. 2 (d). The diameter of the VSJ is 50 mm and the length 65 mm.

C. VSL and VSJ pressure actuation system

To control the stiffness of the variable stiffness components, the inner air pressure of the VSL and the two silicone-based chambers of the VSJ are independently controlled. Each pressure control system consists of a proportional pressure regulator (Camozzi K8P-0-E522-0, $0 \sim 3$ bar, $0 \sim 10$ v) and a voltage regulator controlled by a pulse-width modulation (PWM) signal to supply $0 \sim 10$ v voltage to the pressure regulator. The entire system has also a 24 v power source for the regulators and a compressor supplying a minimum of 3 bar air pressure, as well as an NI PC-based Data Acquisition (DAQ) to provide the PWM to the voltage regulator while receiving the pressure feedback from the pressure regulator. This system manages the air pressures inside the VSL and VSJ silicone-based chambers, leading to a change in their stiffness.

For the VSJ, one pressure regulator is connected to each of the silicone-based chambers. By controlling the difference in pressure for each chamber, a bending angle of the rotational hinge can be achieved. Also, the stiffness of the VSJ can be varied by inflating both chambers at the same time.

D. Combination of various link and joint components resulting in four joiny-link units (JLUs)

To fully assess and compare the stiffness, load capacity, and repetitive accuracy of joint-link units, four sets of units have been composed as shown in as shown in 1: a Dynamixel XM430 servo motor and a rigid link manufactured by the SLS 3D printing process with the material of Nylon PA2200 (JLU 1) representing the traditional rigid JLU of collaborative robots, a motor joint and VSL (JLU 2), a VSJ and a rigid link (JLU 3) as well as a VSJ and VSL (JLU 4). For JLU 1, the XM430-W350 servo motor (DYNAMIXEL, CA, USA) has a stall torque of 4.1 N.m (at 12 V, 2.3 A). Safety requirements limit the maximum driving current to 1.1 A. The height of the servo motor is 46.5 mm, the width is 28.5 mm and the length 34 mm. Comparing the the heights between the servo motor and VSJ, the height of the VSJ is 1.39 times the height of the motor. The dimension of the rigid link is the same as the VSL, which is 40 mm in diameter and 100 mm in length.

Using a combination of the VSL, VSJ, a rigid link and the commercially available servo motor, we assembled four types of JLUs, which are JLU 1 (motor and rigid link), JLU 2 (motor and VSL), JLU 3 (VSJ and rigid link) and the JLU 4 (VSJ and VSL) respectively, as shown in Fig. 1.

III. EXPERIMENTS, RESULTS AND DISCUSSION

Three experiments have been conducted to investigate the stiffness, output force and repetitive accuracy and characterize the performance of the four types of different JLUs. In the following section, we report on the experimental protocol and results, aiming to understand the influence of the VSL and VSJ on JLUs.

A. Experimental protocol and setup

1) Experiment 1 - stiffness evaluation: To characterize the change in stiffness for the set of JLUs, all four units are set to their highest stiffness mode. For the VSL and VSJ, the pressure values for the maximum stiffness have been empirical determined. A summary of the settings for the joints (either the servo motor or the VSJ) and links (either the rigid link or the VSL) used in experiment 1 and 2 is shown in Table I. Then, weights from 0 N to 10 N are mounted on the end of each JLU. As shown in Fig. 3 (a), an Aurora 3D tracking system (NDI Intl. Ontario¡ CA), an electromagnetic position tracking system, is used to monitor the tip position during these loading processes. The deflection of the end will indicate the stiffness of four types of units.

2) Experiment 2 - output force evaluation: For characterizing the change in the output force for each JLUs, the tip of each unit is placed on a Force/Torque (F/T) sensor (by IIT, Genova, Italy) as shown in Fig. 3 (b). Depending on the JLU, the motor or VSJ are then actuated to the

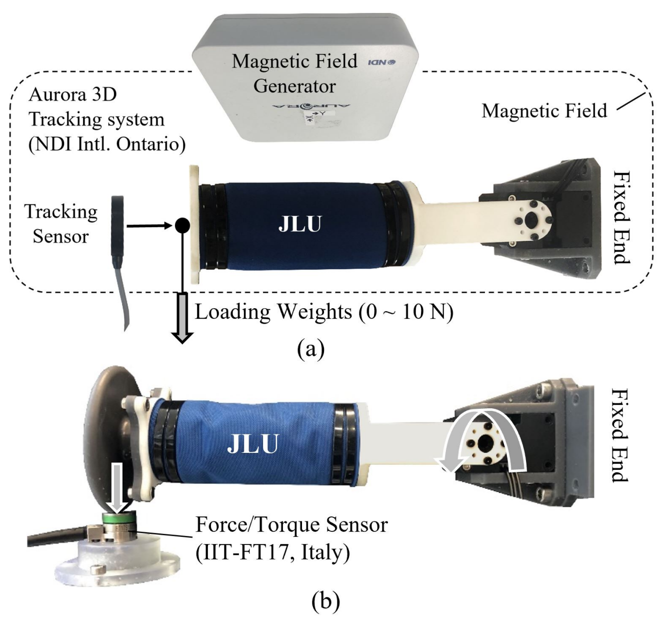

Fig. 3. (a) Setup for experiment 1: The base of the JLU is fixed to a platform with an Aurora magnetic tracking sensor mounted on its tip. The tracked change of position represents the deflection of the JLU's tip when a set of weights from 0N to 10N with intervals of 2N are loaded on the unit end. Hence, the stiffness of the unit can be determined. (b) Setup for experiment 2: The base of the JLU is fixed to a platform, while the end of the unit is attached to a Force/Torque (F/T) sensor by a circular connector. When the actuators of the JLUs drives the rotational motion anticlockwise, the end of the JLUs will exert a force on the F/T sensor. This recorded force is the output force of the JLUs.

TABLE I

SETTINGS OF PRESSURES AND CURRENT FOR JLU COMPONENTS DURING EXPERIMENT 1 AND 2

Experiment 1		
	Joint	**Link**
JLU 1	Dynamixel XM430 motor: stall torque mode/1100 mA current	Rigid link
JLU 2	Dynamixel XM430 motor: stall torque mode/1100 mA current	VSL: 1 bar internal pressure
JLU 3	VSJ: 2 bar/2 bar internal pressure of two chambers	Rigid link
JLU 4	VSJ: 2 bar/2 bar internal pressure of two chambers	VSL: 1 bar internal pressure
Experiment 2		
	Joint	**Link**
JLU 1	XM430 motor actuation current: 0 mA ∼ 1100 mA	Rigid link
JLU 2	XM430 motor actuation current: 0 mA ∼ 1100 mA	VSL: 0.25 bar/ 0.5 bar/ 0.75 bar/ 1 bar internal pressure
JLU 3	VSJ actuation pressure: 0 bar ∼ 2 bar	Rigid link
JLU 4	VSJ actuation pressure: 0 bar ∼ 2 bar	VSL: 0.25 bar/ 0.5 bar/ 0.75 bar/ 1 bar internal pressure

maximum output torque (i.e. 1100 mA current or 2 bar in air pressure, respectively), while the inner pressure of the VSL is incrementally increased from 0.25 bar to 1 bar by 0.25 bar steps. The summary of the settings for experiment 2 is shown in Table I. Thus, the force generated by the four JLUs is recorded by the F/T sensor.

3) Experiment 3 - accuracy and repeatability evaluation: For characterizing the influence of the repeatability and accuracy of the JLUs, a combination of experiment 1 and 2 are used to evaluate the accuracy and repeatability with regards to the position and force. For the repeatability and accuracy test of the position, the four JLUs are repetitively actuated from 10° to 40° in 10° steps. This experiment is run 30 times for each JLU. To determine the repeatability and accuracy with regards to the force, the output current of the motor in JLU 1 and JLU 2 is set as 200 mA, 400 mA, 600 mA, and 800 mA, while the pressure of the actuation chamber in JLU 3 and JLU 4 is set as 0.5 bar, 1 bar, 1.5 bar, and 2 bar. All force tests were carried out 30 times each as well.

B. Experiments results

1) Results for experiment 1 - stiffness evaluation: As shown in Fig. 4, the red and blue curve show the deflection of JLU 1 and 2, where the actuation current in both two motors is 1.1 A. Both of these two curves seem linear. The green and yellow curve show the deflection of JLU 3 and 4, where the actuation pressure in both VSJs is 2 bar. These two curves show a non-linear behavior with a similar tendency. The link pressure in the VSLs is 1 bar in all cases. The shaded area of each curve represents the error distribution of the recorded deflections. For JLU 1 and 2, the error distribution is small and neglectable. For JLU 3 and 4, however, the error distribution increases and then descreases again for loads between 4 N and 8 N. The results of the stiffness evaluation show that the maximum deflection of the four JLUs' tips is 13.5 mm, 21.6 mm, 99.1 mm and 104.4 mm, respectively when our maximum load of 10 N is applied. Compared to JLU 1, the deflection of JLU 2 is 1.6 times higher, the deflection of JLU 3 is 7.3 times larger, and the one of JLU 4 is 7.7 times higher. It can be concluded that the VSL decreases only marginally the stiffness values compared to the rigid link. However, the VSJ can just achieve one-seventh of the stiffness values of the motor. In addition, the curves of JLU 4 and 3 in Fig. 4 show a non-linear behavior, while the curves of JLU 1 and 2 show a linear tendency. Hence, the VSJ results in non-linearity of the JLU behavior.

2) Results for experiment 2 - output force evaluation: In Fig. 5 (a), the red curve shows the output force of JLU 1. The other four curves show the output force from JLU 2 with 1 bar, 0.75 bar, 0.5 bar and 0.25 bar internal pressure of VSL. The maximum output force of JLU 1 is 8.74 N, while the maximum output force of JLU 2 supplied with different pressure values are 8.17 N, 7.98 N, 7.76 N, 6.32 N. In Fig. 5 (b), the red curve shows the output force of JLU 3. The other four curves show the output force from JLU 4 with 1 bar, 0.75 bar, 0.5 bar and 0.25 bar internal pressure of the VSL. The maximum output force of JLU 3 is 13.62 N, while the maximum output force of of JLU 4 with different pressure values applied to the VSL are 12.78 N, 12.51 N, 12.32 N, 11.78, N. The shade of each curve illustrates the error distribution of the recorded forces. From the results of

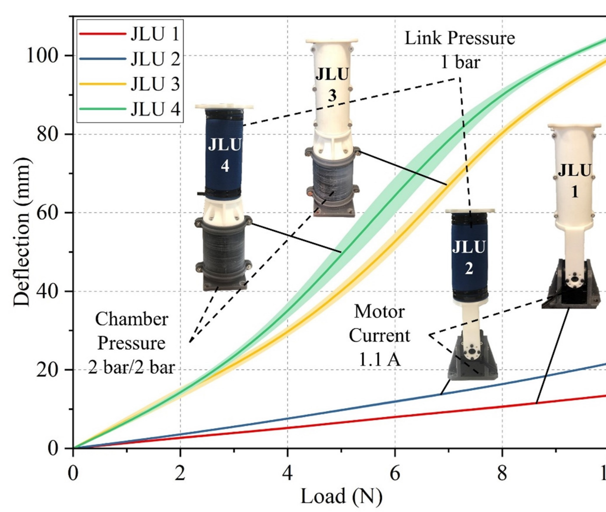

Fig. 4. Results of experiment 1: The red curve and blue curve show the deflection of the JLUs 1 and 2. The actuation current in both motors is 1.1 A. The green and yellow curve show the deflection of the JLU 3 and 4, where the actuation pressure in both VSJs is 2 bar. In all cases, the link pressure in the VSLs is 1 bar.

the output forces, it can be seen that the VSJ can achieve a higher output force than the Dynamixel XM430 motor (i.e. the maximum output force from VSJ is 1.55 times the maximum output force of the motor). Also, comparing the forces generated by JLU 3 and 4 inflated with different internal pressure (i.e. 1 bar, 0.75 bar, 0.5 bar, 0.25 bar), it is observed that the output forces from JLU 4 are 0.93, 0.91, 0.9, 0.86 times of the force from JLU 3, respectively. It can be concluded that the VSL will decrease the output force of the unit slightly, in particular at sufficiently high pressure values (i.e., 1 bar).

3) Results for experiment 3 - repeatability and accuracy: In Figs. 6 and 7, the box plots show the distribution of the bending angles and forces when the four JLUs are moved 30 times. For the position repeatability and accuracy plot in Fig. 6, (a)-(d) show the data for JLU 1-4, respectively. Here, JLU 1 shows the highest accuracy, where the bending angle fluctuates within 0.1°, irrespectively of the value of the bending angle. The bending angle of JLU 2 fluctuates within 0.13°. For JLU 3, however, the maximum error range becomes 0.5°. JLU 4 has the lowest position accuracy - the maximum error reaches around 4° at 40° bending angle. It can be concluded that the accuracy decreases through the introduction of the VSL (by 2 to 8 times) and VSJ (by 5 to 30 times) into the kinematic chain.

From Fig. 7, it can be observed that the repetitive forces generated by JLU 1 and 2 have similar error ranges (i.e. from 0.1 N to 0.5 N) when the motor current is 200 mA, 400 mA, 600 mA and 800 mA. However, the error ranges of the forces from JLU 3 and 4, reaching from 0.1 N to 1.2 N, are slightly larger compared to the ones from JLU 1 and 2. So, the VSJ decreases the repetitive accuracy of the force. The error range becomes up to 2 times larger compared to the error resulting from experiment with the servo motor. Further, there seems to be no difference in error range between JLU 1 and 2 as well as between JLU 3 and 4. Hence, the VSL has no negative effect on the force accuracy.

C. Discussion

Firstly, comparing the VSL at 1 bar inner pressure with the rigid link in the stiffness evaluation testing (experiment 1), the maximum deflection of JLU 2 is 1.6 times larger than the one of JLU 1, while the maximum deflection of JLU 4 is 1.05 times that of JLU 3. In other words, the decreased rate of stiffness of the VSL is 37.5% and 5.1%. Considering the inherent disadvantages of soft materials, the decreased rate of stiffness seems acceptable and the VSL can achieve a similar level of stiffness as the rigid link in a high-pressure state. Looking at the output force results (experiment 2), the maximum output force from JLU 2 with a 1 bar inner pressure inside the VSL is about 0.93 times the force

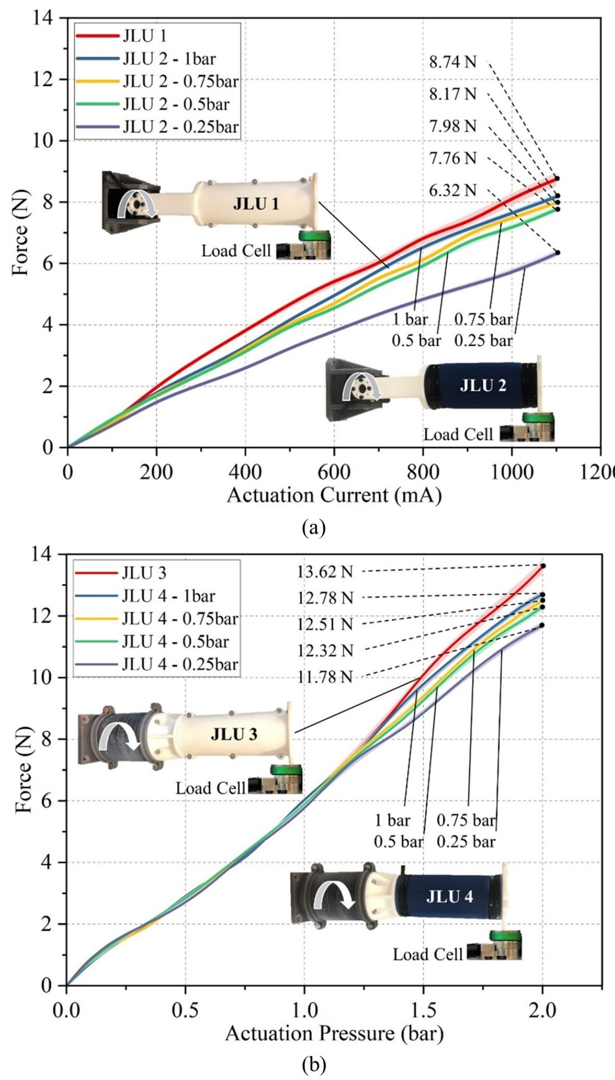

Fig. 5. Results for experiment 2: The red curve shows the output force of (a) JLU 1 and (b) JLU 3. The other four curves show the output forces from (a) JLU 2 and (b) JLU 4 with 1 bar, 0.75 bar, 0.5 bar and 0.25 bar internal pressure of the VSL.

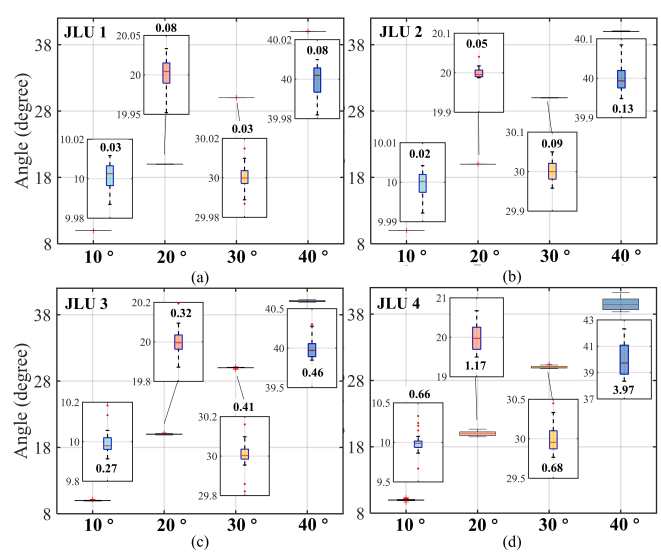

Fig. 6. Results for experiment 3: Boxplot for the repeatability and accuracy with regards to the position for (a) JLU 1, (b) JLU 2, (c) JLU 3 and (d) JLU 4. The bending angle of the JLUs are set to 10°, 20°, 30° and 40°. Each JLU is actuated 30 times.

TABLE II
SUMMARY OF THE RELATIVE COMPARISON RESULTS

Components	Max Stiffness	Max Output Force	Repetitive Position Accuracy				Repetitive Force Accuracy			
			10°	20°	30°	40°	1	2	3	4
Rigid Link (Nylon PA2200)	1	1	0.66	0.62	1	1	0.44	1	1	0.59
VSL (1 bar inner pressure)	0.62 ∼ 0.95	0.93 ∼ 0.94	1	1	0.33	0.61	1	0.84	0.99	1
Servo Motor (XM430)	1	0.64 ∼ 0.65	1	1	1	1	0.56	1	1	1
VSJ (2 bar actuation pressure)	0.14 ∼ 0.21	1	0.11	0.25	0.07	0.17	1	0.5	0.26	0.88

generated by JLU 1. The output force from JLU 4 with a 1 bar inner pressure inside the VSL is 0.94 times the force generated by JLU 3. Hence, the VSL has a very small influence (a 6% to 7% decrease in output force) on the maximum output force.

Secondly, from the repeatability and accuracy results (experiment 3), it is evident that the position error of JLU 1 and 2 both remain around 0.1 mm. The position error of JLU 3 and 4 increase to around 0.4 mm and 1 mm, respectively. In particular, the error reaches 3.97 mm when JLU 4 is actuated to 40°. Hence, a VSL alone does not increase the overall position error. A combination of a VSL and VSJ, however, returns an additional position error of about 3.97 mm. This rather larger error might result from an error superposition of measurement errors and mechanical errors of the two variable stiffness systems introduced in the JLU. Looking at the results of the repetitive force accuracy, JLU 1 and 2 have similar levels of force errors of about 0.25 N, while JLU 3 and 4 have have a similar level of circa 1 N.

Overall, the VSL prototype in this paper shows a 5.1% to 37.5% decreased rate in stiffness values and a 6% to 7% decreased rate in output force when compared to a rigid link. When the joint is a servo motor, experiments with the VSL achieve nearly the same repetitive position accuracy compared to experiments with a VSJ (when the position error is around 2 times larger) and almost the same repetitive force accuracy. Comparing the VSJ with the servo motor in the stiffness evaluation (experiment 1), the deflection of JLU 3 is 7.3 times larger than that of JLU 1, while the deflection of JLU 4 is 4.8 times higher than that of JLU 2. Hence, the VSJ has a significant effect on the overall stiffness when compared to the servo motor. In terms of output force, the the opposite statement can be concluded: the output force applied by JLU 3 is 1.55 times larger compared to JLU 1, and the force applied by JLU 4 is 1.56 times higher than JLU 2. Hence, the VSJ can generate more force (around 1.5 times more) than the servo motor (at the applied current values). Looking at the repetitive accuracy, the position error from JLU 3 and 4 is around $5-10$ times larger than the error of JLU 1 and 2, while the force error from JLU 3 and 4 is around 2 times larger than the error of JLU 1 and 2.

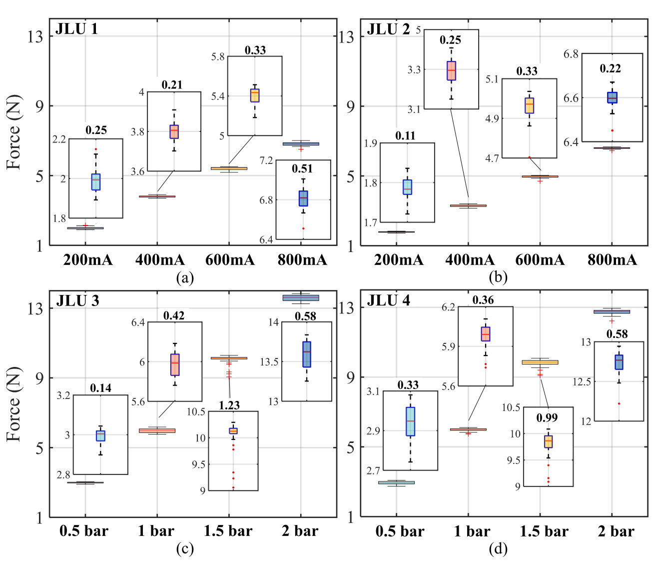

Fig. 7. Results for experiment 3: Boxplot for the repeatability and accuracy with regards to forces for (a) JLU 1, (b) JLU 2, (c) JLU 3 and (d) JLU 4. The current of the servo motor for JLU 1 and 2 is set to 200 mA, 400 mA, 600 mA and 800 mA. The current of the motor for JLU 3 and 4 is set to 0.5 bar, 1 bar, 1.5 bar and 2 bar. Each JLU is actuated 30 times.

The servo motor can achieve 4.8 to 7.3 times larger stiffness values compared to the VSJ. However, the VSJ can achieve 1.5 times larger output forces. Furthermore, the repetitive position error of the VSJ is 5 to 10 times higher compared to the servo motor, while the repetitive force error is 1 to 2 times higher. A detailed comparison of the results is presented in Table II, where the best values for each characteristic are set as 1 and any value below these are presented as percentages of the corresponding best values.

IV. CONCLUSIONS

This paper characterizes joint-link units (JLUs) made of a combination of a variable stiffness link (VSL) and joint (VSJ) as well as servo motor and rigid link. Experimental results show that the VSL has minor differences in terms of stiffness (0.62 ∼ 0.95), output force (0.93 ∼ 0.94) and repetitive accuracy compared to a rigid link. Hence, a VSL has great potential to replace a rigid link without a significant decrease in performance. For the VSJ, experimental results show that there is a significant difference in the performance of the servo motor in terms of maximum stiffness (0.14 ∼ 0.21) and repetitive position accuracy (0.07 ∼ 0.25). Nonetheless, it can be concluded that a similar performance with regards to repetitive force accuracy and better performance with regards to the maximum output force (1.54 ∼ 1.55 times) can be achieved. Future works include creating advanced VSJs and multi-degree-of-freedom cobots made of the presented JLUs.

REFERENCES

[1] D. Rus and M. T. Tolley, "Design, fabrication and control of soft robots," *Nature*, vol. 521, pp. 467–475, 5 2015.

[2] M. Li, A. Pal, A. Aghakhani, A. Pena-Francesch, and M. Sitti, "Soft actuators for real-world applications," *Nature Reviews Materials 2021 7:3*, vol. 7, pp. 235–249, 11 2021.

[3] S. Wolf, G. Grioli, O. Eiberger, W. Friedl, M. Grebenstein, H. Hoppner, E. Burdet, D. G. Caldwell, R. Carloni, M. G. Catalano, D. Lefeber, S. Stramigioli, N. Tsagarakis, M. Van Damme, R. Van Ham, B. Vanderborght, L. C. Visser, A. Bicchi, and A. Albu-Schaffer, "Variable Stiffness Actuators: Review on Design and Components," *IEEE/ASME Transactions on Mechatronics*, vol. 21, pp. 2418–2430, 10 2016.

[4] C. Gaz, M. Cognetti, A. Oliva, P. R. Giordano, and A. de Luca, "Dynamic identification of the Franka Emika Panda Robot with retrieval of feasible parameters using penalty-based optimization," *IEEE Robotics and Automation Letters*, vol. 4, pp. 4147–4154, 10 2019.

[5] S. Wolf, T. Bahls, M. Chalon, W. Friedl, M. Grebenstein, H. Höppner, M. Kühne, D. Lakatos, N. Mansfeld, M. Can Özparpucu, F. Petit, J. Reinecke, R. Weitschat, and A. Albu-Schäffer, "Soft robotics with variable stiffness actuators: Tough robots for soft human robot interaction," *Soft Robotics*, pp. 231–254, 1 2015.

[6] G. Grioli, S. Wolf, M. Garabini, M. Catalano, E. Burdet, D. Caldwell, R. Carloni, W. Friedl, M. Grebenstein, M. Laffranchi, D. Lefeber, S. Stramigioli, N. Tsagarakis, M. Van Damme, B. Vanderborght, A. Albu-Schaeffer, and A. Bicchi, "Variable stiffness actuators: The user's point of view:," *The International Journal of Robotics Research*, vol. 34, pp. 727–743, 3 2015.

[7] M. Manti, V. Cacucciolo, and M. Cianchetti, "Stiffening in soft robotics: A review of the state of the art," *IEEE Robotics and Automation Magazine*, vol. 23, pp. 93–106, 9 2016.

[8] H. A. Wurdemann, A. Stilli, and K. Althoefer, "An Antagonistic Actuation Technique for Simultaneous Stiffness and Position Control," *Lecture Notes in Computer Science*, vol. 9246, pp. 164–174, 2015.

[9] G. Yang, B. Li, Y. Zhang, D. Pan, and H. Huang, "A Novel Soft Wrist Joint with Variable Stiffness," in *International Conference on Intelligent Robotics and Applications*, pp. 346–356, Springer, Cham, 2022.

[10] Q. Ruan, F. Yang, H. Yue, Q. Li, L. Li, and R. Liu, "A Ball Joint With Continuously Adjustable Load Capacity Based on Positive Pressure Method," *IEEE Robotics and Automation Letters*, vol. 7, pp. 8415–8422, 7 2022.

[11] A. Stilli, H. Wurdemann, and K. Althoefer, "A Novel Concept for Safe, Stiffness-Controllable Robot Links," *Soft Robotics*, vol. 4, pp. 16–22, 3 2017.

[12] A. Stilli, L. Grattarola, H. Feldmann, H. A. Wurdemann, and K. Althoefer, "Variable Stiffness Link (VSL): Toward inherently safe robotic manipulators," in *IEEE International Conference on Robotics and Automation*, pp. 4971–4976, Institute of Electrical and Electronics Engineers Inc., 7 2017.

[13] T. Morrison and H. J. Su, "Stiffness modeling of a variable stiffness compliant link," *Mechanism and Machine Theory*, vol. 153, p. 104021, 11 2020.

[14] L. Gao, Y. He, H. Zhu, G. Sun, and L. Zhu, "Stiffness modelling and performance evaluation of a soft cardiac fixator flexible arm with granular jamming," *Machines*, vol. 9, 12 2021.

[15] M. Su, R. Xie, Y. Zhang, X. Kang, D. Huang, Y. Guan, and H. Zhu, "Pneumatic Soft Actuator with Anisotropic Soft and Rigid Restraints for Pure in-Plane Bending Motion," *Applied Sciences*, vol. 9, p. 2999, 7 2019.

[16] G. Bao, S. Cai, Z. Wang, S. Xu, P. Huang, Q. Yang, F. Xu, and L. Zhang, "Flexible pneumatic robotic actuator FPA and its applications," in *IEEE International Conference on Robotics and Biomimetics*, pp. 867–872, IEEE Computer Society, 2013.

[17] L. Paternò, G. Tortora, and A. Menciassi, "Hybrid Soft–Rigid Actuators for Minimally Invasive Surgery," *Soft Robotics*, vol. 5, pp. 783–799, 12 2018.

[18] P. Ohta, L. Valle, J. King, K. Low, J. Yi, C. G. Atkeson, and Y. L. Park, "Design of a Lightweight Soft Robotic Arm Using Pneumatic Artificial Muscles and Inflatable Sleeves," *Soft Robotics*, vol. 5, pp. 204–215, 4 2018.

[19] L. Hao, C. Xiang, M. E. Giannaccini, H. Cheng, Y. Zhang, S. Nefti-Meziani, and S. Davis, "Design and control of a novel variable stiffness soft arm," *Advanced Robotics*, vol. 32, pp. 605–622, 6 2018.

[20] H. Karoline, "BionicSoftArm Lifts and Grips Like Nature Intended," *Fluid Power Journal*, vol. 28, no. 1, pp. 16–17, 2021.

[21] J. M. Gandarias, Y. Wang, A. Stilli, A. J. Garcia-Cerezo, J. M. Gomez-De-Gabriel, and H. A. Wurdemann, "Open-loop position control in collaborative, modular variable-stiffness-link (VSL) robots," *IEEE Robotics and Automation Letters*, vol. 5, pp. 1772–1779, 4 2020.